Theor. Exp. Plant Physiol. (2025) 37:23
https://doi.org/10.1007/s40626-025-00365-4

Intermittent UV-B irradiation optimizes secondary metabolite production and growth in red rubin basil

Awais Ali · Piero Santoro · Jacopo Mori · Antonio Ferrante · Giacomo Cocetta

Received: 17 March 2024 / Accepted: 8 January 2025

Abstract Understanding the plant growth responses and secondary metabolite synthesis to artificial ultraviolet-B irradiation (UV-B) is important for selecting the crop, UV-B doses, wavelength, and exposure time for the application. Red rubin basil was grown in a glasshouse under supplemental LED lights and periodically irradiated with artificial 4 W UV-B lamp at a single wavelength of 315 nm, in an indoor UV-B chamber for 3 h and 6 h. These treatments resulted in cumulative UV-B of 43.2 kJ m^{-2} and 86.4 kJ m^{-2} respectively. Both UV-Bs improved the overall production, indicating a significant potential of artificial UV-B in development and improvement of red rubin basil. A thiobarbituric acid reactive substance (TBARS) assay was carried out to assess the membrane oxidative damage to basil plants after the UV-B treatments. The results showed significant higher lipid peroxidation in UV-B treated basil in relation to control plants. Significantly increased concentrations of carotenoids was found for 43.2 kJ m^{-2} UV-B compared to 86.4 kJ m^{-2} while similar chlorophyll a and b concentrations were observed for 43.2 kJ m^{-2} UV-B compared to both 86.4 kJ m^{-2} and control. *In vivo* analysis revealed an increase of flavanols under post 86.4 kJ m^{-2} UV-B while the overall leaf performance index significantly reduced under this UV-B. The maximum quantum efficiency of photosystem II declined for both UV-B treatments compared to the control while a significant increment was seen in terms of absorption and dissipation of heat on active reaction centers in post UV-B 86.4 kJ m^{-2} compared to post 43.2 kJ m^{-2} UV-B. Similarly, significant increment in phenolic index and total anthocyanins concentrations was seen for 86.4 kJ m^{-2} UV-B treated plants. The UV-B of 86.4 kJ m^{-2} exhibited a significant higher nitrate concentration compared to the control. Furthermore, the basil under 43.2 kJ m^{-2} UV-B significantly outperformed other treatments in terms of reducing sugars and sucrose while 86.4 kJ m^{-2} treated plants yielded lower total sugars between the treatments. The present findings provided an insight

A. Ali (✉) · G. Cocetta
Department of Agricultural and Environmental Sciences, Universita Degli Studi Di Milano, via Celoria, 2, 20133 Milan, MI, Italy
e-mail: awais.ali@unimi.it

G. Cocetta
e-mail: giacomo.cocetta@unimi.it

P. Santoro
MEG Science., via Aleardo Aleardi 12, 20154 Milan, MI, Italy
e-mail: santoro@megscience.com

J. Mori
ALMECO S.p.A., Via della Liberazione 15, 20098 Civesio di S. Giuliano Milanese, MI, Italy
e-mail: jacopo.mori@almecogroup.com

A. Ferrante
Institute of Crop Science, Scuola Superiore Sant'Anna, Piazza Martiri della Libertà, 33, 56127 Pisa, PI, Italy
e-mail: antonio.ferrante@unimi.it; antonio.ferrante@santannapisa.it

Published online: 03 April 2025

into how artificial UV-B could potentially affect the accumulation of phytochemical compounds.

Graphical abstract

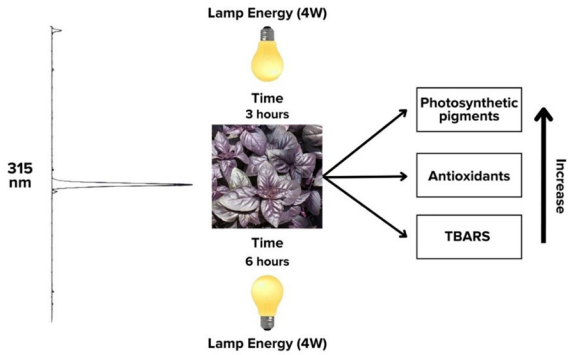

Keywords Antioxidants · Carotenoids · Chlorophyll fluorescence · Lipid peroxidation · Secondary metabolites · UV-B elicitors

1 Introduction

The ultraviolet radiation can be divided into three ranges: UV-C (100–280 nm), UV-B (280–315 nm), and UV-A (315–400 nm). Among these, UV-B radiation is one of the most important environmental light elements affecting plant growth and development (Heijde and Ulm 2012). Plants are exposed to UV-B radiation from both natural sunlight and artificial sources such as fluorescent lamps, which can cause genetic alterations, DNA damage, or cell death (Bhusal et al. 2021). In addition, the damaging effects of UV-B radiation on organisms are continuously worsened by stratospheric ozone dynamics and climate change (Bornman et al. 2019). It is well known that exposure to UV-B radiation can inhibit plant growth and development by directly or indirectly generating a number of negative effects such as it alters the activation, expression, and subsequent translation of genes involved in the phenylpropanoids biosynthesis pathway, including chalcone synthase (*CHS*), flavanol synthase (*FLS*), damage repair photolyase 1 (*PHR1*), and UV repair defective 3 (*UVR3*) (Heijde and Ulm 2012).

The effects of UV-B on plants are regulated by a variety of mechanisms including the formation of phytochemicals that serve various functions, such as defense against herbivores, attraction of pollinators, and protection from environmental stress (Fig. 1). Some important photo-protectants that absorb UV-B light and assist plants against irradiation damage include tocopherols, phenolic compounds, carotenoids, anthocyanins, and flavonoids (Khaleghi et al. 2019). Plants employ a UV-B-specific signaling pathway, in response to UV-B radiation, using cytosolic UVR8 photoreceptors that go through a series of processes to control the genes that produce the phenylpropanoid pathway enzymes such as phenylalanine ammonia lyase (*PAL*) (EC. 4.3.1.24), *CHS* (EC. 2.3.1.74), and *FLS* (EC 1.14.20.6) and help plants acclimatize to UV-B (Heijde and Ulm 2012). On the other hand, plants perform a non-specific UV-B signaling response that aids in UV-B shielding and acclimation by accumulating reactive oxygen species (ROS) and phytohormones such as jasmonic acid, salicylic acid, nitric oxide, and ethylene, which are later involved in the overexpression of stress-related genes such as pathogenesis-related 1, 2 and 5 (*PR-1*, *PR-2*, and *PR-5*) and the plant defensin 1.2 gene

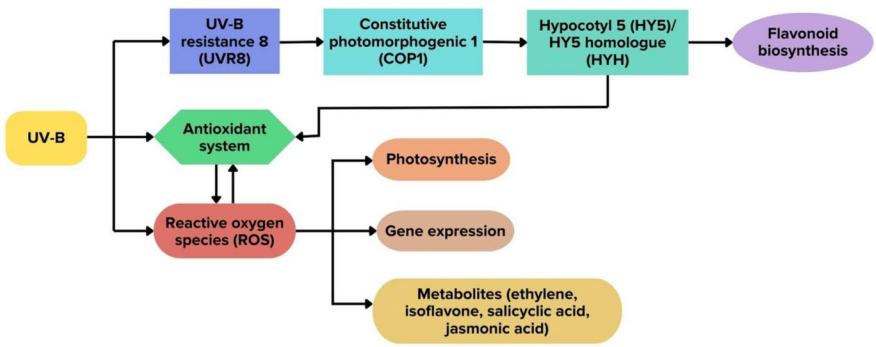

Fig. 1 Schematic diagram representing the mechanism of plant responses towards ultraviolet B irradiation

(*PDF1.2*) (Cisneros-Zevallos et al. 2014). UV-B induces morphological, physiological, and molecular changes in plants (Ali et al. 2023a). Previous studies have highlighted several morphological changes in plants, including the inhibition of hypocotyl elongation, reduction in root growth, biomass, stem elongation, overall crop yield, fertility, internode shortening, and increased leaf thickness in plants (Crestani et al. 2022). Reduction in Rubisco activity and photosynthesis, degradation of photosystem II, accumulation of ROS, UV protective pigments and antioxidants, photooxidation of indole acetic acid (IAA), and peroxidation of lipids are some of the physiological effects caused by UV-B radiation in plants (Chen et al. 2022). Furthermore, UV-B is responsible for the induction of repair mechanisms, stimulation of homologous recombination, downregulation of photosynthetic genes, and formation of cyclobutene pyrimidine dimers (CPDs) in plants (Soni et al. 2022).

Basil is a fast-growing crop which contains essential oils, phenolics, flavonoids, and phenylpropanoids, which provide basil with a distinct flavor and aroma (Ferrarezi and Bailey 2019). Basil can be grown in a variety of target markets, including medicines, ornamental plants, culinary uses, and fresh or dry spices (Walters and Currey 2015). Purple basils are grown for culinary and tea because of their potential as source of anthocyanins and their antioxidant characteristics (Ferrarezi and Bailey 2019). Based on previous results in green basil, such as increased total sugars, phenolic index as well as reduced total chlorophyll, anthocyanins and nitrates (Ali et al. 2023d), we hypothesized that the red rubin basil will behave differently under the same UV-B irradiances. Moreover, despite being conspecific, the two varieties may exhibit differential responses to UV irradiation as purple-leaved varieties are characterized by improved anthocyanin accumulation and are also known to possess enhanced photoprotective mechanisms, particularly against UV radiation. Moreover, after evaluating the physiological results, we will be able to select a potential UV-B value for enhancing the secondary metabolite productions in the red rubin basil for future production. Thus, in this study, we evaluated the artificial UV-B stress on red rubin basil after irradiating it with two UV-B values and by investigating the accumulation of secondary metabolites in response to the respective UV-Bs.

2 Material and methods

2.1 Plant material

Red rubin basil (*Ocimum basilicum* 'Purpurascens') seeds were sown in pots filled with a peat-based substrate (VIGORPLANT SUPERNUTRIENTE ORTAGGI SRL, Italy). Cultivation took place in an experimental glasshouse of Department of Agricultural and Environmental Sciences, University of Milan Italy, under monitored growing conditions: temperature 24.3 ± 0.03 °C, relative humidity $62.7 \pm 0.12\%$. Illumination was provided by natural light, with an average light intensity of 101.7 ± 0.9 µmole m^{-2} s^{-1} during the day with the addition of supplemental LED lights (Dutch lighting instruments: DLI DIODE-Series Top Lighting Fixture 400W) with an average photosynthetic photon flux density (PPFD) of 65 µmole m^{-2} s^{-1} and photoperiod of 16 h (Fig. 2). The plants were fertilized and irrigated regularly, and the UV-B treatments were carried out in a closed UV-B chamber.

2.2 UV-B exposure to red rubin basil

For UV-B treatments, an indoor UV chamber (Philips UV Broadband TL 40W/01 RS) equipped with an aluminium reflector realized with vega® UV, a physical vapour deposition (PVD) surface was used which was specifically developed to optimize the reflectance in the UV bandwidth of wavelength 315 nm (Fig. 3).

The UV-B chamber was placed in a room located in closed proximity to the glasshouse. It was made up of three compartments separated from each other by a thick wooden cardboard, capable of independent operation (Fig. 4). One of the compartments held the control plants (so they could be kept overnight without receiving UV-B therapy), and the other two held the plants for corresponding UV-B treatments 86.4 kJ m^{-2} and 43.2 kJ m^{-2}, which were performed overnight with an automatic on and off mode in order to delay the senescence effects in darkened leaves when followed by the illumination (Sztatelman et al. 2015).

The time scheme for the UV-B application was set according to the Table 1. When the basil plants ($n = 6$) were 10–12 cm in height, a day (only on Tuesday night) per week of UV-B treatment for three weeks consecutively, from a 4W UV-B source

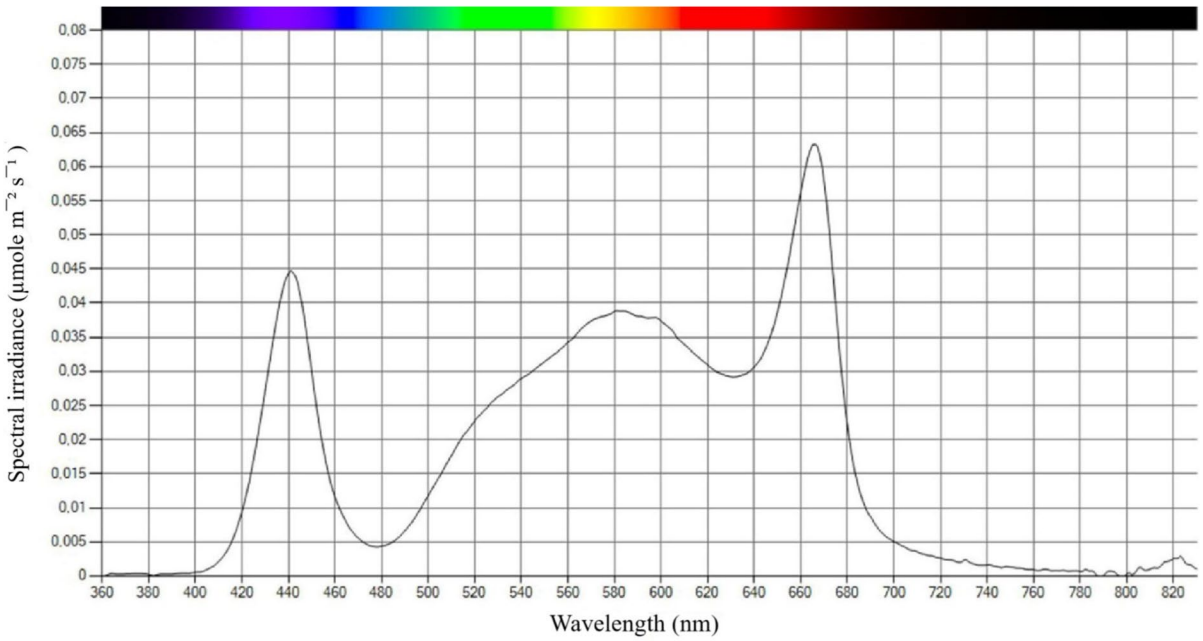

Fig. 2 Spectral quantum distribution used in glasshouse for red rubin basil (R: 77.1%; G + Y:17.9%; B: 5%)

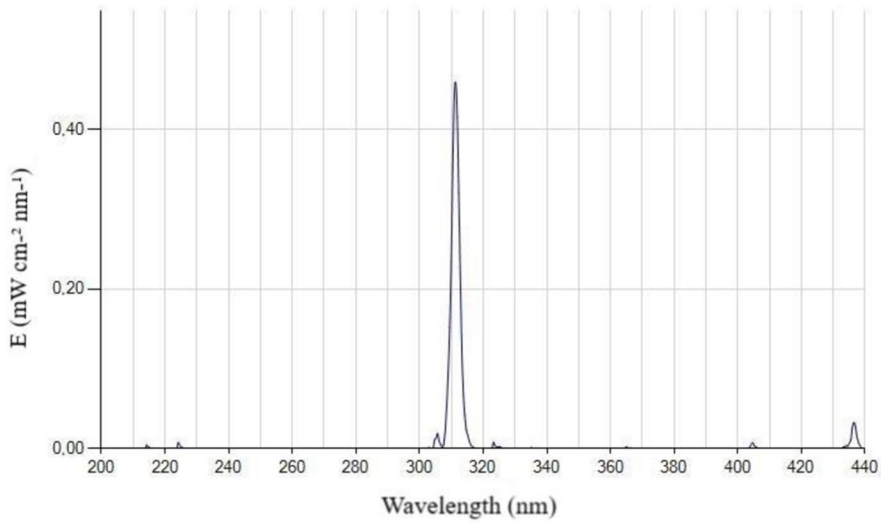

Fig. 3 Spectrum of the UV-B lamps. A single wavelength of 315 nm was used on the red rubin basil plants

was administered, for the total time exposure of 6 h and 3 h per day for cumulative 86.4 kJ m^{-2} and 43.2 kJ m^{-2} UV-B respectively. The plants were harvested 35 days after sowing,

2.3 Fresh mass and water content

The red rubin basil plants were harvested from the base using scissor and weighed using a digital scale (Mettler PM480 Delta Range) to investigate the fresh mass of the produce. The water content, expressed as a percentage (%), was estimated by allowing four plants from

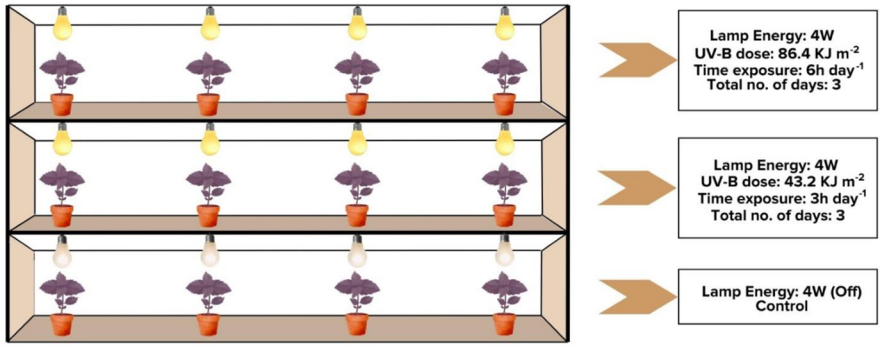

Fig. 4 Diagrammatic representation of UV-B chamber used; it consisted of three horizontal chambers, capable of independent operations. The top chamber hosted plants for the 86.4 kJ m^{-2} UV-B exposure. The middle chamber for 43.2 kJ m^{-2} UV-B while the bottom compartment had control plants with UV-B lamps off

Table 1 Time scheme for an automatic UV-B treatments of both UV-B 43.2 kJ m^{-2} and 86.4 kJ m^{-2} to red rubin basil. For 43.2 kJ m^{-2}, treatment started at 20:00 pm and lasted for 30 min after which there was an off phase for next 1 h:30 min. The treatment started again at 22:00 pm for another 30 min UV-B exposure followed by 1 h: 30 min off-phase and so on until 06:30 am for a total of 180 min or 3 h of UV-B treatment. For 86.4 kJ m^{-2}, starting time was 20:00 pm and UV-B exposure of 1 h was applied to red rubin basil after which there is an off-phase of 1 h. UV-B treatment started again at 22:00 pm for 1 h until 23:00 followed by a 1 h off-phase and so on until 07:00 am for total of 360 min or 6 h of UV-B treatment

UV-B 43.2 kJ m^{-2}			UV-B 86.4 kJ m^{-2}		
ON	OFF	Minutes	ON	OFF	Minutes
20:00	20:30	30	20:00	21:00	60
22:00	22:30	30	22:00	23:00	60
00:00	00:30	30	00:00	01:00	60
02:00	02:30	30	02:00	03:00	60
04:00	04:30	30	04:00	05:00	60
06:00	06:30	30	06:00	07:00	60
		Total: 3 h			Total:6 h

each condition to dry in an oven (VENTICELL, VC 707 ECO) for three days at a temperature of 110 °C. After this drying period, the dry mass (DM) of the plants was measured, and the water loss (WL%) was calculated as follows:

$$WL\% = 100 - \left(\frac{DW}{FW} \cdot 100\right)$$

2.4 Non-destructive analyses

2.4.1 In vivo estimation of chlorophyll, flavanols and anthocyanins

Before and after each UV-B application, as well as at harvest, chlorophyll, flavonols and anthocyanin concentrations were measured in vivo using MPM-100 Multipigment meter (ADC BioScientific Ltd, UK) (Cerovic et al. 2008). Adaxial surfaces of fully matured leaves were selected for the fluorescence detection to measure the above-mentioned parameters (n = 7).

2.4.2 Chlorophyll a fluorescence

Leaves light utilization and health status of photosystem II was observed by chlorophyll *a* fluorescence which was estimated on dark adapted (30 min) matured red rubin basil leaves (n = 7) using a portable fluorimeter (Handy PEA; Hanstech, Kings Lynn, UK). Subsequently, leaf tissues were exposed to a saturating light (3000 µmol m^{-2} s^{-1}) for 1 s from an array of three high-intensity light-emitting diodes. The maximum quantum efficiency of photosystem II (Fv/Fm), leaf fluorescence performance index (PI), absorption per active reaction center (ABS/RC) and dissipation energy per active reaction center (DIo/RC) were evaluated. These analyses provided information about the relative leaf functionality. The intensity of active reaction centres (RCs), the efficiency of electron transport and the probability that an absorbed photon will be trapped by the RCs are usually considered while describing the overall leaf performance index.

2.5 Analytical measurements

2.5.1 Total chlorophylls and total carotenoids

Fresh matured leaf tissues (around 50 mg) in 5 mL of 99.9% methanol were used to determine the total chlorophylls and carotenoids. Leaf tissues were placed in methanol and resultant were placed at 4 °C for 24 h in a dark room. Absorbance readings were measured at 665.2 nm and 652.4 nm for chlorophyll pigments while for total carotenoids at 470 nm with Evolution 300 UV–Vis spectrophotometer (Thermo Scientific). Lichtenthaler's formula was followed for the calculation of chlorophyll and carotenoid concentrations (Lichtenthaler 1987).

2.5.2 Phenolic index and total anthocyanins

Around 50 mg of matured leaves were treated with 5 mL of acidified methanol (1% HCl v/v) and left overnight in the dark for the extraction. The phenolic index, which represented the total phenolic concentrations, was calculated as the absorbance measured at 320 nm using an Evolution 300 UV–Vis spectrophotometer (Thermo Scientific) (Ke and Saltveit 1989). The same extracts were used for the analytical measurements of anthocyanins where the concentration was expressed as cyanidin-3-glucoside equivalents and determined spectrophotometrically at 535 nm using an extinction coefficient εM of 29,600 (Ferrante et al. 2004).

2.5.3 Thiobarbituric acid reactive substances (TBARS)

Lipid peroxidation was assessed by using the thiobarbituric acid reactive substances (TBARS) method to assess any possible photodamage to the membranes (Heath and Packer 1968). One gram of leaf tissue, which were stored at − 80 °C was ground in 5 mL of trichloroacetic acid (TCA) of 0.1% w/v. The resultant mixture was centrifuged (ALC centrifuge-model PK130R) at 4000 rpm for 10 min. In the next step, one mL of the extract was mixed with 4 mL of 20% (w/v) TCA, 25 L of 0.5% thiobarbituric acid (TBA) including distilled water. The extract was heated at 95 °C for 30 min in a Dubnoff bath (PID) after mixing and later cooled in ice. The absorbance at 600 nm was subtracted from the reading at 532 nm (as an index of non-specific turbidity) and the concentration of TBARS were expressed as malondialdehyde (MDA) equivalents (nmol g^{-1} FM), with the extinction coefficient $\varepsilon M = 155\ mM^{-1}\ cm^{-1}$.

2.5.4 Nitrate concentration

Cataldo's method was used to assess the nitrate concentration (Cataldo et al. 1975). Roughly 1 g of leaves samples were taken and ground in 4 mL of distilled water. At 4000 rpm for 15 min, the extract was centrifuged (ALC centrifuge-model PK130R) and the supernatant was recovered. This supernatant was later used for the colorimetric determination of nitrate and sugars.

Twenty µL of the sample was added to 80 µL of 5% salicylic acid in sulphuric acid (H_2SO_4) and to 3 mL of 1.5 N sodium hydroxide (NaOH). The samples were cooled at room temperature. The spectrophotometric readings were recorded at 410 nm. The nitrate concentrations were estimated based on a potassium nitrate (KNO_3) standard calibration curve (0–10 mM).

2.5.5 Total sugars, reducing sugars and sucrose concentrations

The supernatants previously prepared for nitrates was used for these analyses. 0.2 mL of leaf extract was mixed with 0.2 mL of 2 M NaOH, after which the mixture was incubated in a water bath (Dubnoff bath (PID) at 100 °C for 10 min. Hot resorcinol buffer at 1.5 mL (containing 30% hydrochloric acid, 1.2 mM resorcinol, 4.1 mM thiourea 1.5 M acetic acid) was added to samples and incubated at 80 °C for another 10 min in the water bath. The samples were cooled at room temperature. After cooling, the optical density was determined at 500 nm and a sucrose standard curve (0–2 mM) was used for calculating the final concentration (Rorem et al. 1960).

For reducing sugars, 0.2 mL of extract was added to 0.2 mL of a solution containing 62.6 mM dinitrosalicylic acid (DNS) and 1.52 M potassium sodium tartrate (Miller 1959). The reaction mixture was heated at 100 °C for 5 min. In the next step, 1.5 mL of distilled water was added in the mixture, and absorbance was measured at 530 nm using spectrophotometer. Glucose standard curve

(0–4 mM) as glucose equivalent, was used to expressed reducing sugars concentration in the sample.

The anthrone method with slight modifications was used to determine the total sugars (Yem and Willis 1954). The anthrone reagent (10.3 mM) was prepared dissolving anthrone in ice-cold 95% H_2SO_4. In the next step, 0.5 mL of extract was placed on top of 2.5 mL of anthrone reagent and kept in ice for 5 min. The mix was vortexed vigorously and heated at 95 °C for 10 min and left to cool in ice. Readings were performed at 620 nm and total sugars concentration was calculated, based on a glucose calibration (0–4 mM).

Evolution 300 UV–Vis spectrophotometer (Thermo Scientific) was used to carry out spectrophotometric determinations.

2.6 Data analysis

Data were subjected to a one-way analysis of variance (ANOVA) followed by Tuckey's test with multiple comparisons for the destructive analyses performed. However, for fluorimeter data and MPM-100 multi-pigment meter readings, two-way analysis of variance (ANOVA) was carried out with Tukey post-test with multiple comparison. Analyses were performed using GraphPad Prism version 6 for Windows (GraphPad Software; La Jolla, California, USA, www.graphpad.com).

3 Results

3.1 Fresh mass and water content

Both average fresh mass and water content were significantly affected by 86.4 kJ m^{-2} UV-B compared to the control. As UV-B irradiation increased, a subsequent increase in production was observed (Fig. 5a). The UV-B 86.4 kJ m^{-2} yielded (11.11 g), a significant 50% increase in production compared to the control (7.39 g). The 43.2 kJ m^{-2} did not significantly affect fresh mass (9.69 g). In terms of water content, the highest UV-B, 86.4 kJ m^{-2} significantly resulted in an increased water content, while the 43.2 kJ m^{-2} UV-B exhibited a non-significant intermediate value compared to the control and the highest UV-B dose (Fig. 5b).

3.2 Non-destructive estimation of chlorophyll, flavanols and anthocyanins

In vivo non-destructive estimation of chlorophyll, flavanols, and anthocyanins was carried out using an MPM-100 Multi-pigment-Meter. No significant differences in chlorophyll values were observed among the UV-B treatments and the control before and after UV-B application as shown in Table 2. Significant reduced flavanols were found in 86.4 kJ m^{-2} compared to post UV-B, control and 43.2 kJ m^{-2} and later enhanced in post UV-B treatment. However, no significant increments were observed among UV-B

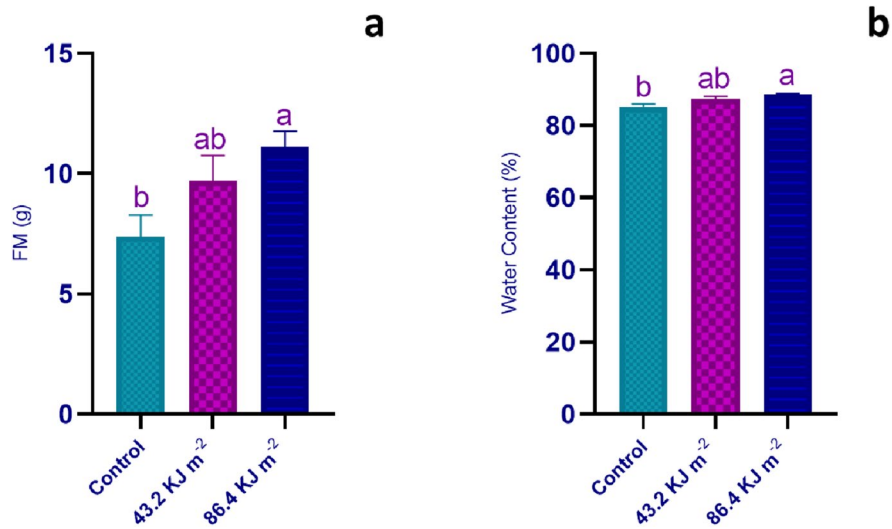

Fig. 5 Fresh mass (**a**) Water content (**b**) recorded in red rubin basil treated with 43.2 kJ m^{-2}, 86.4 kJ m^{-2} UV-B, and control. Values are mean (n = 4 ± S.E). Different letters indicate significant differences among treatments after one way ANOVA followed by Tukey multiple comparison test ($p < 0.05$)

Table 2 Non-destructive estimation of chlorophyll, flavanols and anthocyanins in red rubin basil recorded through MPM-100 Multi-pigment meter

Treatments	Data Recording (time)	Chlorophyll T850/T720 nm	Flavanols F660/F325 nm	Anthocyanin F660/F225 nm
Control	No UV-B	0.49 ± 0.06^{ns}	0.46 ± 0.04^{a}	0.33 ± 0.01^{ns}
	No UV-B	0.51 ± 0.06^{ns}	0.50 ± 0.03^{a}	0.31 ± 0.008^{ns}
43.2 kJ m^{-2}	Pre UV-B	0.42 ± 0.07^{ns}	0.47 ± 0.05^{a}	0.26 ± 0.02^{ns}
	Post UV-B	0.49 ± 0.09^{ns}	0.56 ± 0.04^{a}	0.30 ± 0.03^{ns}
86.4 kJ m^{-2}	Pre UV-B	0.55 ± 0.17^{ns}	0.22 ± 0.02^{b}	0.20 ± 0.04^{ns}
	Post UV-B	0.47 ± 0.10^{ns}	0.57 ± 0.02^{a}	0.25 ± 0.04^{ns}

All values are expressed as mean ± standard error (n = 7). Different alphabetic letters indicate the significant differences among the values after two-way ANOVA followed by Tukey multiple comparison test ($p < 0.05$)

application and control in terms of anthocyanins estimated values.

3.3 Chlorophyll fluorescence

As per Table 3, Under UV-B stress, a significant decline of Fv/Fm in post UV-B application was seen in 86.4 kJ m^{-2} UV-B treatment that showed a significant decline in the leaf PI as well. Notably, a significantly higher ABS/RC was recorded at post 86.4 kJ m^{-2} UV-B compared to pre 43.2 kJ m^{-2} UV-B. The DIo/RC was non-significant between the pre and post UV-B treatment of 86.4 kJ m^{-2}, however, the DIo/RC in post UV-B of 86.4 kJ m^{-2} was significantly higher compared to other pre and post treatments.

3.4 Analytical measurements of red rubin basil for 43.2 kJ m^{-2} and 86.4 kJ m^{-2} UV-B

Non-significant increase in the chlorophyll concentrations of 43.2 kJ m^{-2} was observed (12.77 µg mg^{-1}) compared to the (10.96 µg mg^{-1}) of control and (10.68 µg mg^{-1}) of 86.4 kJ m^{-2} (Fig. 6a). Similarly, a significant increment in the concentration of carotenoid pigment (1.692 µg mg^{-1}) was observed in 43.2 kJ m^{-2} compared to the (1.075 µg mg^{-1}) of 86.4 kJ m^{-2} UV-B (Fig. 6b). Carotenoids concentration in control (1.495 µg mg^{-1}) however, were non-significant compared to both 86.4 kJ m^{-2} and 43.2 kJ m^{-2} UV-B.

A significant increase in the phenolic index (Fig. 7a) was recorded in 86.4 kJ m^{-2} compared to 43.2 kJ m^{-2} UV-B and control. Being the highest accumulated phenolic index of (69.20 ABS_{320} g^{-1} FM) in 86.4 kJ m^{-2} UV-B, it was recorded (34.96 ABS_{320} g^{-1} FM) in control and (34.36 ABS_{320} g^{-1} FM) for 43.2 kJ m^{-2} UV-B respectively. Likewise phenolic index, a significant anthocyanin concentration (101.5 Cyanidin 3-glucoside eq. mg 100 g^{-1} FM), was observed under 86.4 kJ m^{-2} UV-B compared to (58.14 Cyanidin 3-glucoside eq. mg 100 g^{-1} FM) in control. Non-significant differences, however,

Table 3 Non-destructive estimation of Fv/Fm, PI, ABS/RC and DIo/RC of red rubin basil recorded through fluorimeter

Treatments	Data Recording (time)	Fv/Fm	PI	ABS/RC	DIo/RC
Control	No UV-B	0.80 ± 0.1^{a}	1.68 ± 0.35^{b}	0.67 ± 0.02^{ab}	0.39 ± 0.03^{b}
	No UV-B	0.76 ± 0.01^{a}	1.59 ± 0.35^{ab}	0.69 ± 0.02^{ab}	0.45 ± 0.04^{b}
43.2 kJ m^{-2}	Pre UV-B	0.71 ± 0.03^{a}	1.74 ± 0.39^{ab}	0.60 ± 0.03^{b}	0.48 ± 0.04^{b}
	Post UV-B	0.75 ± 0.01^{a}	1.32 ± 0.31^{ab}	0.66 ± 0.07^{ab}	0.39 ± 0.03^{b}
86.4 kJ m^{-2}	Pre UV-B	0.79 ± 0.007^{a}	0.83 ± 0.16^{ab}	0.76 ± 0.07^{ab}	0.76 ± 0.18^{ab}
	Post UV-B	0.52 ± 0.05^{b}	0.74 ± 0.20^{a}	0.94 ± 0.08^{a}	1.92 ± 0.63^{a}

The values are expressed as mean ± standard error (n = 7). Different alphabetic letters indicate the significant differences among the values after the two-way ANOVA followed by Tukey multiple comparison test ($p < 0.05$)

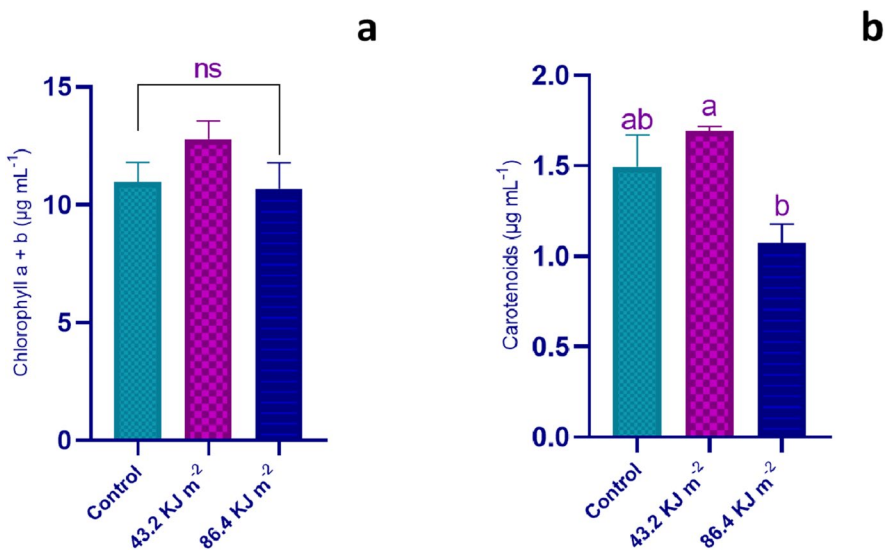

Fig. 6 Chlorophyll a + b (**a**) Carotenoids (**b**) concentrations recorded in red rubin basil treated with 43.2 kJ m^{-2} and 86.4 kJ m^{-2} UV-B and control. Values are mean (n = 4 ± S.E). Different letters indicate significant differences among treatments after one way ANOVA followed by Tukey multiple comparison test ($p < 0.05$)

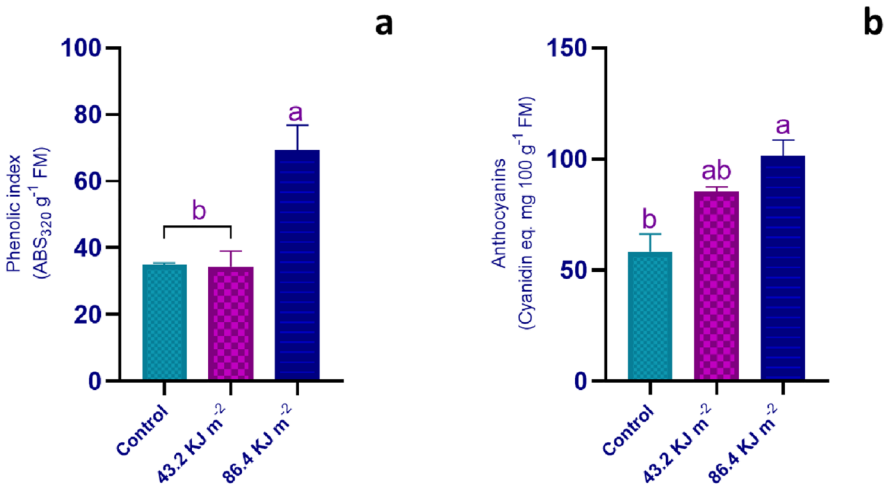

Fig. 7 Phenolic Index (**a**) Anthocyanins (**b**) concentrations recorded in red rubin basil treated with 43.2 kJ m^{-2}, 86.4 kJ m^{-2} UV-B and control. Values are mean (n = 4 ± S.E). Different letters indicate significant differences among treatments after one way ANOVA followed by Tukey multiple comparison test ($p < 0.05$)

were recorded in 43.2 kJ m^{-2} (85.20 Cyanidin 3-glucoside eq. mg 100 g^{-1} FM) (Fig. 7b).

TBARS assay was performed to assess the possible oxidative damage caused by the UV-B to the membranes. A significant increase in malonaldehyde was observed in both UV-Bs compared to the control however, the increment was non-significant among the UV-B treatments (Fig. 8a). The control demonstrated the lowest TBAR value of (7.806 nmol MDA g^{-1} FM) against the (28.57 nmol MDA g^{-1} FM) and (42.74 nmol MDA g^{-1} FM) of 43.2 kJ m^{-2} and 86.4 kJ m^{-2} UV-Bs respectively. Furthermore, the control exhibited the significant lowest nitrate concentration (106 mg Kg^{-1}) compared to the (176.9 mg Kg^{-1}) of 86.4 kJ m^{-2}. The UV-B 43.2 kJ m^{-2} was, however, non-significant and intermediate in nitrate concentration (147.6 mg Kg^{-1}), compared to the other two treatments (Fig. 8b).

The UV-B treatment of 43.2 kJ m^{-2} and control yielded a significantly higher total sugar compared to the 86.4 kJ m^{-2} UV-B. The recorded total sugar of (1.428 mg Glu eq g^{-1} FM) in the control and (1.432 mg Glu eq g^{-1} FM) under the 43.2 kJ m^{-2} was significantly higher than (1.036 mg Glu eq g^{-1} FM) of 86.4 kJ m^{-2} (Fig. 9a). For sucrose concentrations, non-significant variations were seen among control (0.28 mg g^{-1}) and 86.4 kJ m^{-2} (0.28 mg g^{-1}) however, the UV-B 43.2 kJ m^{-2} turned out the treatment with significantly highest accumulated sucrose among all the treatments at (0.52 mg g^{-1}) (Fig. 9b).

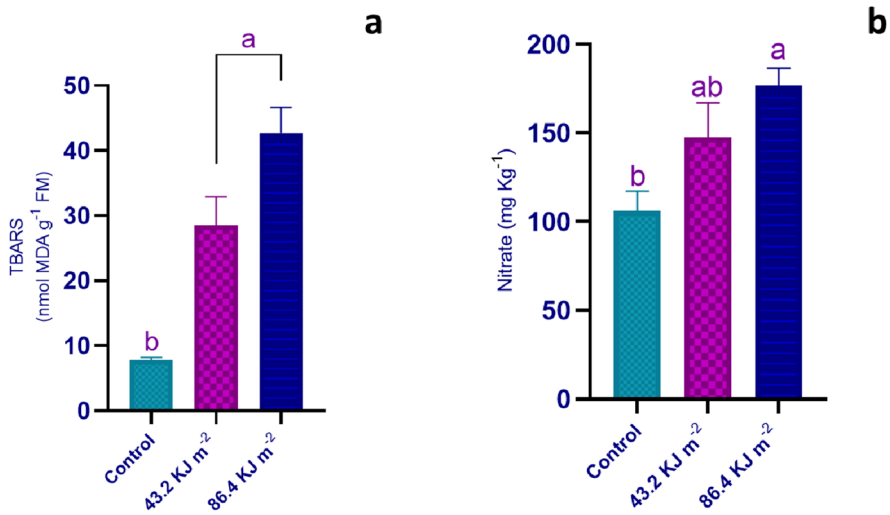

Fig. 8 TBARS (**a**) Nitrate (**b**) concentrations recorded in red rubin basil treated with 43.2 kJ m^{-2}, 86.4 kJ m^{-2} UV-B and control. Values are mean (n = 4 ± S.E). Different letters indicate significant differences among treatments after one way ANOVA followed by Tukey multiple comparison test ($p < 0.05$)

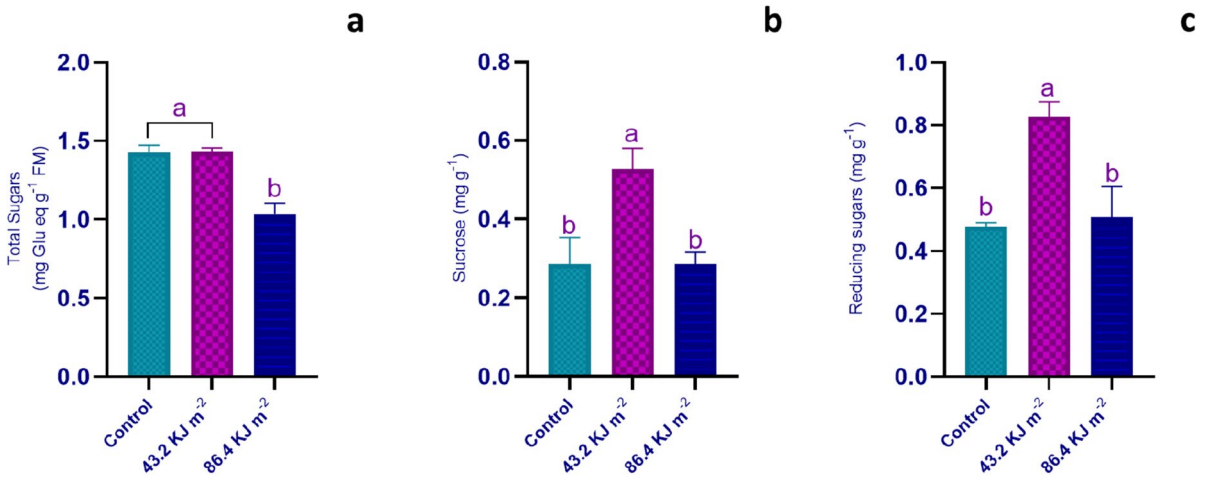

Fig. 9 Total sugars (**a**) Sucrose (**b**) Reducing sugar (**c**) concentrations recorded in red rubin basil treated with 43.2 kJ m^{-2}, 86.4 kJ m^{-2} UV-B and control. Values are mean (n = 4 ± S.E). Different letters indicate significant differences among treatments after one way ANOVA followed by Tukey multiple comparison test ($p < 0.05$)

Like sucrose, a similar trend was observed for the reducing sugars with control being the lowest (0.477 mg Kg^{-1}), 86.4 kJ m^{-2} being the next (0.50 mg Kg^{-1}) and the recorded highest reducing sugar concentration (0.82 mg Kg^{-1}) for the 43.2 kJ m^{-2} respectively (Fig. 9c).

4 Discussion

UV radiation, a naturally occurring component of solar radiation, is a significant environmental element that influences plant growth and development. UV-B has always been regarded as a stressor that can seriously harm plants. However, the regulatory qualities of low, ecologically significant UV-B irradiances have come to light in terms of unique modifications that lead to the accumulation of plant secondary metabolites (Schreiner et al. 2016). Moreover, the

effect of UV-B on plant chemistry is transient and time-dependent (Hectors et al. 2014). The photosynthetic pigment concentrations such as chl a and b in red rubin basil were not significantly affected by the UV-B radiation values applied of the present study (Fig. 6a). Usually, UV-B is known for the reduction of these pigments in the plants as it damages the chloroplasts followed by the degeneration of photosystem II and the activation of senescence-related genes (Salama et al. 2011). However, according to our previous findings in wild rocket, an increased chlorophyll a and b accumulations under UV-B of 21.6 kJ m^{-2} potentially explained the UV-B effects as dependent on UV-B values and species (Ali et al. 2023b). The increase in chlorophyll and improved photosynthesis are generally not attributed to UV-B. But the choice of crop, UV-B irradiance, and exposure time should be carefully monitored to obtain the best effects of UV-B in terms of photosynthetic pigment accumulation (Jovanić et al. 2022; Xie et al. 2022). Plants produce carotenoids, such as carotenes and xanthophylls which assist them in protecting chlorophyll from photooxidation, eliminating reactive oxygen species, and harnessing light (Shen et al. 2018). Several genes such as *PSY*, *LCY-E*, *LCY-b*, *CHY-b*, and *VDE*, are crucial for the accumulation of these accessory photosynthetic pigments. However, their specific regulatory role in carotenoid accumulation is still unknown (Toledo-Ortiz et al. 2010). Increased accumulation of total carotenoids under UV-B of 43.2 kJ m^{-2} possibly protected the red rubin basil's photosynthetic machinery from photooxidation which helped the plant to avoid photosystem II degeneration which was otherwise quite prominent under 86.4 kJ m^{-2} UV-B (Fig. 6b). Increased basil production for this study under UV-B treatments contradicts the previously studied UV-B results and its potential effects on the yield (Surabhi et al. 2009). However, increased production of accessory pigments could be the reason for the intact photosynthetic apparatus in which the UV-B assisted plants in upregulation of the expression of genes that encodes the array of defense mechanisms and helped in pigment protection that eventually led to higher production in UV-B treated plants. Also, the intermittent application of UV-B irradiation with dark periods may have created an environment where the plants were able to tolerate the UV-B exposure and even benefitted from it. Therefore, an increased fresh mass in the present study could be a result of the plants' ability to effectively adapt to the UV-B stress and utilize the energy provided by the radiation for growth. Similarly, the plants were grown under continuous supplemental LED lighting, a practice known to promote growth rates and increased biomass production in certain leafy greens such as lettuce (Ali et al. 2023b). Additionally, LED lights, particularly those emitting red and blue wavelengths in higher proportion of the recipe (Fig. 2), are highly effective in stimulating photosynthesis, resulting in elevated photosynthetic rates and increased sugar production. Kim et al. (2024) reported no differences in the biomass of *Achyranthes japonica* Nakai (AJN), with an intermittent UV-B exposures before harvesting and suggested that this mode of UV-B treatments is beneficial for the secondary metabolites production without compromising the production of the crop. In canola seedlings, it has been discovered that UV-B values, such 5 kJ m^{-2} and 10 kJ m^{-2}, resulted in an increase carotenoid accumulation. This suggests the involvement of UV-B specific pathways which are responsible for the activation of UVR8 photoreceptor (Qaderi et al. 2010). Increased in the production of carotenoids such as lutein, shielded wheat endosperm photosystem II from long-term UV-B stress results and improved overall growth and development (Yu et al. 2022). In addition, when subjected to UV-B, red cabbage sprouts, maize kernels, and bell peppers all showed an increase in total carotenoids which provided us the insight that carotenoids act as an accessory pigment under mild UV-B stress to shield the photosynthetic pigment accumulation of the plants and aid in overall photosynthesis (Martínez-Zamora et al. 2021). Notably, under UV-B 86.4 kJ m^{-2}, non-specific signaling cascades linked to severe DNA damage and high ROS production may indirectly affect the production of carotenoids (Jansen et al. 2008).

Additionally, a PSII efficiency value of 0.80 indicates optimal photosynthetic performance. Values below this threshold suggest reduced photosynthetic efficiency, potentially leading to photoinhibition (Xu et al. 2022). Both UV-B treated red rubin basil recorded values lower than the 0.80 which indicated that the plants perceived UV-B as stress and affected the conversion of absorbed light into photochemistry. This is also evident from the higher dissipation of energy and higher number of active absorptions of photons on the reaction center (Table 3). Stressed

plants are believed to exhibit higher ABS/RC which directly reflects the higher density of inactive reaction center and reduced electron transport per reaction center in response to light (Janeeshma et al. 2022) and drought stress such as in lettuce (Franzoni et al. 2021) and quinoa plants (Fghire et al. 2015). These parameters could be the reason for the overall reduced leaf performance index under UV-B irradiated red rubin basil. UV-B and UV-C irradiances are known to adversely affect the performance of photosystem II. However, Fv/Fm values under UV-B are known to be more affected than those under UV-C, for example, in almonds Fv/Fm values are recorded as low as 0.75, which were caused by an increased chloroplast damage and disturbed photosynthesis (Ranjbarfordoei et al. 2011).

Most of the research in recent years has focused on understanding how UV-B exposure affects plant phenolic components such as flavones, flavanols, iso-flavonoids, anthocyanins, and phenolic acids (Heijde and Ulm 2012; Schreiner et al. 2012). The UV-responsive transcription factors HY5 and PFG1/MYB12 control the expression of phenols and flavonoid genes during UV response in plants. These genes include chalcone synthase (*CHS*), chalcone isomerase (*CHI*), *FLS*, dihydroflavonol 4-reductase (*DFR*), and *PAL* (Gai et al. 2022). Both in vitro as well as in vivo analysis revealed that UV-B successively induced higher phenolic index, flavanols and anthocyanins in red rubin basil with the successive increase in the cumulative UV-B values (Table 2, Fig. 7a, b). This indicated that as a barrier against exposure to solar UV-B radiation, phenolic compounds are typically concentrated on the outer surfaces of the plants and help them against the abiotic stress (Soobrattee et al. 2005). In our earlier research (Ali et al. 2023c, 2023a), it was discovered that the cumulative UV-B of 43.2 kJ m^{-2} in spearmint (*Mentha spicata*) and both 43.2 kJ m^{-2} and 21.6 kJ m^{-2} in wild rocket (*Diplotaxis tenuifolia*) were beneficial in increasing antioxidant production. Despite different UV-B irradiances, crops, and exposure times, one aspect of all the experiments was the enhanced secondary metabolite profile which was again observed in this study. Nevertheless, the formation of flavonoids and flavonoids glycosides is more sensitive to UV-B than the formation of phenolic acids, indicating that not all phenolic compounds are generated equally under UV-B stress (Schreiner et al. 2012). Similarly in Canola (*Brassica napus*), artificial UV-B light should be used to increase the synthesis of phytochemicals in the plant sector, but the UV irradiation and wavelength must be considered carefully (Lee et al. 2022).

TBARS assay data (Fig. 8a) demonstrated a positive correlation between UV-B exposure and lipid peroxidation in basil. This is because UV-B is responsible for increasing production of free radicals and reactive oxygen species, which ultimately resulted in increased lipid peroxidation of the membranes in terms of malonaldehyde formation. However, the degree of antioxidant response to UV irradiation is dependent on its irradiance, duration, and the plant genotype response. Notably, in tomato leaves and roots following UV-B exposure, it was found that different plant parts responded in different ways. For example, while the lipid peroxidation in leaves increased by 18%, the roots did not exhibit any detrimental effects (Mannucci et al. 2020). A study on *Artemisia annua* recorded a 25% increase in malonaldehyde (Rai et al. 2011), a by-product of lipid peroxidation that appears consistent to current findings regarding lipid peroxidation in red rubin basil. Additionally, for normal growth and activities, plants store excess nitrates in the leaves for proper leaf functioning against UV-B stress and along with sugars use it for the formation of amino acids and proteins in secondary metabolism. An increase in the nitrate accumulation was observed in the successive increase in the UV-B compared to the control (Fig. 8b), which is in line with the finding where a buildup of 14.49 times more nitrates in the shoots was observed under UV-B due to enhanced activity of the nitrate transporter (*NRT1.8*) (Wang et al. 2022). In response to UV-B irradiation, there is a trigger to produce reactive oxygen species (ROS) which activates nitrate reductase *(NR)* which later takes part in the conversion of nitrates to nitrites and nitric oxide *(NO)* (Wang et al. 2022). For this study, increasing nitrates are the indication of less of the above said conversion which might be due to the disruptive *NR* activity under UV-B values. The formation of NO is important for inducing the phenylpropanoid pathway that initiates the action of *CHS* and *CHI* genes which eventually result in UV-B acclimation and protection (Gupta et al. 2011).

In addition to being an essential part of the defense mechanism against biotic and abiotic stress and a regulator of growth and development, sugars also

interact with signaling molecules, including phytohormones that regulate every stage of plant development and growth, including embryogenesis, control of organ size, pathogen defense, stress tolerance and reproductive development (Ciereszko 2018). A considerable increment in reducing sugars, sucrose and total sugars was observed under 43.2 kJ m^{-2} UV-B, marking it as a potential UV-B value with an effective UV-B exposure time for enhancing the sugar profile of red rubin basil (Fig. 9a–c). A similar study on white clover went in line with our findings in which total sugars, reducing sugars and starch increased in both roots and leaves in response to UV-B irradiation (Hamid et al. 2022). Likewise, UV-B treatment at 1.4 kJ m^{-2} d^{-1} in peach fruits potentially induced the expression of sugar transporter genes and assisted in facilitating the accumulation of 1.5 times more total sugars (Wang et al. 2018). Moreover, sugar accumulations and enhanced antioxidants accumulation somehow helped the plants in neutralizing the negative impact of UV-B application. An increment in Douglas-fir *(Pseudotsuga menziesii)* herb output and biomass explained that apart from its general detrimental effect, UV-B effects are crop and time exposure dependent (Torres et al. 2021).

5 Conclusion

UV-Bs in the present study such as 43.2 and 86.4 kJ m^{-2} resulted in enhanced secondary metabolites in the red rubin basil compared to the control. The intermittent application of UV-B irradiation, combined with dark periods, facilitated the development of UV-B tolerance in plants and enabled them to harness the energy from the radiation for enhanced growth. While 86.4 kJ m^{-2} UV-B, for intermittent 6 h irradiance, can be suitable for improved secondary metabolite profile and significant average fresh mass compared to the control, the 43.2 kJ m^{-2} UV-B, on the other hand, resulted in significant improved sucrose and reducing sugars. Therefore, future research efforts should consider the influence of UV-B irradiation timing on the physiological responses of indoor red rubin basil plants.

Acknowledgements Authors would like to thank the efforts of Noramon Tantashutikun for designing graphical abstract and schematic diagram of UV-B responses in plants.

Author contributions AA, GC: structured the experimental concept. AA: conducted the experiments, analyzed the data and wrote the manuscript. GC: assisted in experiments, data analysis, reviewed and edited the manuscript. AF: reviewed and edited the manuscript. PS and JM: designed the UV-B chamber and LED lighting sources for the experiment.

Funding Open access funding provided by Università degli Studi di Milano within the CRUI-CARE Agreement.

Data Availability All data supporting the findings of this study are included in the paper.

Declarations

Conflict of interest The author Piero Santoro was employed by the company MEG Science. The author Jacopo Mori was employed by the company ALMECO. All other authors declare no competing interests.

References

Ali A, Franzoni G, Petrini A, Santoro P, Mori J, Ferrante A, Cocetta G (2023a) Investigating physiological responses of Wild Rocket subjected to artificial ultraviolet B irradiation. Sci Hortic 322:112415. https://doi.org/10.1016/j.scienta.2023.112415

Ali A, Santoro P, Ferrante A, Cocetta G (2023b) Investigating pulsed LED effectiveness as an alternative to continuous LED through morpho-physiological evaluation of baby leaf lettuce (*Lactuca sativa* L. var. Acephala). South Afr J Bot 160:560–570. https://doi.org/10.1016/j.sajb.2023.07.052

Ali A, Santoro P, Mori J, Ferrante A, Cocetta G (2023c) Effect of UV-B elicitation on spearmint's (*Mentha spicata* L.) morpho-physiological traits and secondary metabolites production. Plant Grow Reg. https://doi.org/10.1007/s10725-023-01028-7

Ali A, Santoro P, Mori J, Ferrante A, Cocetta, G (2023d) UV-B irradiation for modulating the quality parameters during postharvest in green basil (Ocimum basilicum L.). In *VII International Conference Postharvest Unlimited* 1396 (pp. 553–560). https://doi.org/10.17660/ActaHortic.2024.1396.73

Bhusal N, Lee M, Lee H, Adhikari A, Han AR, Han A, Kim HS (2021) Evaluation of morphological, physiological, and biochemical traits for assessing drought resistance in eleven tree species. Sci Total Environ 779:146466. https://doi.org/10.1016/j.scitotenv.2021.146466

Bornman JF, Barnes PW, Robson TM, Robinson SA, Jansen MA, Ballaré CL, Flint SD (2019) Linkages between stratospheric ozone, UV radiation and climate change and their implications for terrestrial ecosystems. Photochem Photobio Sci 18(3):681–716. https://doi.org/10.1039/C8PP90061B

Cataldo DA, Maroon M, Schrader LE, Youngs VL (1975) Rapid colorimetric determination of nitrate in plant tissue by nitration of salicylic acid. Commun Soil Sci Plant Anal 6(1):71–80. https://doi.org/10.1080/00103627509366547

Cerovic ZG, Moise N, Agati G, Latouche G, Ghozlen NB, Meyer S (2008) New portable optical sensors for the assessment of winegrape phenolic maturity based on berry fluorescence. J Food Comp Anal 21(8):650–654. https://doi.org/10.1016/j.jfca.2008.03.012

Chen Z, Dong Y, Huang X (2022) Plant responses to UV-B radiation: signaling, acclimation and stress tolerance. Stress Bio 2(1):51. https://doi.org/10.1007/s44154-022-00076-9

Ciereszko I (2018) Regulatory roles of sugars in plant growth and development. Acta Soc Botan Polo. https://doi.org/10.5586/asbp.3583

Cisneros-Zevallos L, Jacobo-Velázquez DA, Pech JC, Koiwa H (2014) Signaling Molecules Involved. Handbook of plant and crop physiology 259.

Crestani G, Cunningham N, Badmus UO, Prinsen E, Jansen MA (2022) UV-B radiation as a novel tool to modulate the architecture of in vitro grown *Mentha spicata* (L.). Agronomy 13(1):2. https://doi.org/10.3390/agronomy13010002

Ferrante A, Incrocci L, Maggini R, Serra G, Tognoni F (2004) Colour changes of fresh-cut leafy vegetables during storage. J Food Agric Environ 2:40–44

Ferrarezi RS, Bailey DS (2019) Basil performance evaluation in aquaponics. HortTech 29:85–93. https://doi.org/10.21273/HORTTECH03797-17

Fghire R, Anaya F, Ali OI, Benlhabib O, Ragab R, Wahbi S (2015) Physiological and photosynthetic response of quinoa to drought stress. Chilean J Agric Res 75(2):174–183. https://doi.org/10.4067/S0718-58392015000200006

Franzoni G, Cocetta G, Ferrante A (2021) Effect of glutamic acid foliar applications on lettuce under water stress. Phys Mol Bio Plants 27:1059–1072. https://doi.org/10.1007/s12298-021-00984-6

Gai QY, Lu Y, Jiao J, Fu JX, Xu XJ, Yao L, Fu YJ (2022) Application of UV-B radiation for enhancing the accumulation of bioactive phenolic compounds in pigeon pea [*Cajanus cajan* (L.) Millsp.] hairy root cultures. J Photochem Photobio B: Bio 228:112406. https://doi.org/10.1016/j.jphotobiol.2022.112406

Gupta KJ, Bauwe H, Mur LA (2011) Nitric oxide, nitrate reductase and UV-B tolerance. Tree Phys 31(8):795–797. https://doi.org/10.1093/treephys/tpr080

Hamid A, Singh S, Agrawal SB (2022) Stage-wise assessment of Trifolium repens performance against elevated UV-B: gaseous exchange, antioxidant and forage quality. Proc Natl Acad Sci India Sect B: Biol Sci 92(2):371–384. https://doi.org/10.1007/s40011-021-01316-0

Heath RL, Packer L (1968) Photoperoxidation in isolated chloroplasts: II. Role of electron transfer. Arch Biochem Biophy 125(3):850–857. https://doi.org/10.1016/0003-9861(68)90523-7

Hectors K, Van Oevelen S, Geuns J, Guisez Y, Jansen MA, Prinsen E (2014) Dynamic changes in plant secondary metabolites during UV acclimation in *Arabidopsis thaliana*. Phys Plant 152(2):219–230. https://doi.org/10.1111/ppl.12168

Heijde M, Ulm R (2012) UV-B photoreceptor-mediated signalling in plants. Trends Plant Sci 17(4):230–237. https://doi.org/10.1016/j.tplants.2012.01.007

Janeeshma E, Johnson R, Amritha MS, Noble L, Aswathi KR, Telesiński A, Puthur JT (2022) Modulations in chlorophyll a fluorescence based on intensity and spectral variations of light. Interl J Mol Sci 23(10):5599

Jansen MA, Hectors K, O'Brien NM, Guisez Y, Potters G (2008) Plant stress and human health: Do human consumers benefit from UV-B acclimated crops? Plant Sci 175(4):449–458. https://doi.org/10.1016/j.plantsci.2008.04.010

Jovanić BR, Radenković B, Despotović-Zrakić M, Bogdanović Z, Barać D (2022) Effect of UV-B radiation on chlorophyll fluorescence, photosynthetic activity and relative chlorophyll content of five different corn hybrids. J Photochem Photobio 10:100115. https://doi.org/10.1016/j.jpap.2022.100115

Ke D, Saltveit ME Jr (1989) Wound-induced ethylene production, phenolic metabolism and susceptability to russet spotting in iceberg lettuce [1-aminocyclopropane-1-carboxylic acid, phenylalanine ammonia-lyase, 2-aminoethoxyvinylglycine, polyphenol oxidase, russet spotting]. Physiologia Plantarum (Denmark). https://doi.org/10.1111/j.1399-3054.1989.tb06212.x

Khaleghi A, Naderi R, Brunetti C, Maserti BE, Salami SA, Babalar M (2019) Morphological, physiochemical and antioxidant responses of *Maclura pomifera* to drought stress. Sci Rep 9(1):1–12. https://doi.org/10.1038/s41598-019-55889-y

Kim YL, Yeom MS, Sim HS, Lee GO, Kang IJ, Yang GS, Son KH (2024) Effect of pre-harvest intermittent UV-B exposure on growth and secondary metabolites in Achyranthes japonica Nakai microgreens in a vertical farm. Horticulturae 10(10):1040. https://doi.org/10.3390/horticulturae10101040

Lee JH, Tanaka S, Goto E (2022) Growth and biosynthesis of phenolic compounds of Canola (*Brassica napus* L.) to different ultraviolet (UV)-B wavelengths in a plant factory with artificial light. Plants 11(13):1732. https://doi.org/10.3390/plants11131732

Lichtenthaler HK (1987) Chlorophylls and carotenoids: pigments of photosynthetic biomembranes. Methods in enzymology. Academic Press, pp 350–382

Mannucci A, Mariotti L, Castagna A, Santin M, Trivellini A, Reyes TH, Quartacci MF (2020) Hormone profile changes occur in roots and leaves of Micro-Tom tomato plants when exposing the aerial part to low doses of UV-B radiation. Plant Phys Biochem 148:291–301. https://doi.org/10.1016/j.plaphy.2020.01.030

Martínez-Zamora L, Castillejo N, Artés-Hernández F (2021) Postharvest UV-B and UV-C radiation enhanced the biosynthesis of glucosinolates and isothiocyanates in Brassicaceae sprouts. Posthar Bio Tech 181:111650. https://doi.org/10.1016/j.postharvbio.2021.111650

Miller GL (1959) Use of dinitrosalicylic acid reagent for determination of reducing sugar. Anal Chem 31(3):426–428

Qaderi MM, Basraon NK, Chinnappa CC, Reid DM (2010) Combined effects of temperature, ultraviolet-B radiation, and watering regime on growth and physiological processes in canola (*Brassica napus*) seedlings. Int J Plant Sci 171(5):466–481. https://doi.org/10.1086/652389

Rai R, Meena RP, Smita SS, Shukla A, Rai SK, Pandey-Rai S (2011) UV-B and UV-C pre-treatments induce physiological changes and artemisinin biosynthesis in *Artemisia annua* L.-An antimalarial plant. J Photochem Photobio B: Biol 105(3):216–225. https://doi.org/10.1016/j.jphotobiol.2011.09.004

Ranjbarfordoei A, Samson R, Van Damme P (2011) Photosynthesis performance in sweet almond [Prunus dulcis (Mill) D. Webb] exposed to supplemental UV-B radiation. Photosynthetica 49:107–111. https://doi.org/10.1007/s11099-011-0017-z

Rorem ES, Walker HG Jr, McCready RM (1960) Biosynthesis of sucrose and sucrose-phosphate by sugar beet leaf extracts. Plant Phys 35(2):269

Salama HM, Al Watban AA, Al-Fughom AT (2011) Effect of ultraviolet radiation on chlorophyll, carotenoid, protein and proline contents of some annual desert plants. Saudi J Bio Sci 18(1):79–86. https://doi.org/10.1016/j.sjbs.2010.10.002

Schreiner M, Mewis I, Huyskens-Keil S, Jansen MAK, Zrenner R, Winkler JB, Krumbein A (2012) UV-B-induced secondary plant metabolites-potential benefits for plant and human health. Crit Rev Plant Sci 31(3):229–240. https://doi.org/10.1080/07352689.2012.664979

Schreiner M, Mewis I, Neugart S, Zrenner R, Glaab J, Wiesner M, Jansen MA (2016) UV-B elicitation of secondary plant metabolites. III-Nitride ultraviolet emitters: technology and applications, pp 387–414. https://doi.org/10.1007/978-3-319-24100-5_14

Shen Y, Li J, Gu R, Yue L, Wang H, Zhan X, Xing B (2018) Carotenoid and superoxide dismutase are the most effective antioxidants participating in ROS scavenging in phenanthrene accumulated wheat leaf. Chemosphere 197:513–525. https://doi.org/10.1016/j.chemosphere.2018.01.036

Soni S, Jha AB, Dubey RS, Sharma P (2022) Application of nanoparticles for enhanced UV-B stress tolerance in plants. Plant Nano Biol. https://doi.org/10.1016/j.plana.2022.100014

Soobrattee MA, Neergheen VS, Luximon-Ramma A, Aruoma OI, Bahorun T (2005) Phenolics as potential antioxidant therapeutic agents: mechanism and actions. Mut Res/fund Mol Mech Mut 579(1–2):200–213. https://doi.org/10.1016/j.mrfmmm.2005.03.023

Surabhi GK, Reddy KR, Singh SK (2009) Photosynthesis, fluorescence, shoot biomass and seed weight responses of three cowpea (*Vigna unguiculata* (L.) Walp.) cultivars with contrasting sensitivity to UV-B radiation. Environ Exp Bot 66:160–171. https://doi.org/10.1016/j.envexpbot.2009.02.004

Sztatelman O, Grzyb J, Gabryś H, Banaś AK (2015) The effect of UV-B on Arabidopsis leaves depends on light conditions after treatment. BMC Plant Biol 15:1–16

Toledo-Ortiz G, Huq E, Rodríguez-Concepción M (2010) Direct regulation of phytoene synthase gene expression and carotenoid biosynthesis by phytochrome-interacting factors. Proc Nat Acad Sci 107(25):11626–11631. https://doi.org/10.1073/pnas.0914428107

Torres R, Romero JM, Lagorio MG (2021) Effects of suboptimal illumination in plants. Comprehensive chlorophyll fluorescence analysis. J Photochem Photobio B: Bio 218:112182. https://doi.org/10.1016/j.jphotobiol.2021.112182

Walters KJ, Currey CJ (2015) Hydroponic greenhouse basil production: comparing systems and cultivars. HortTechnology 25:645–650. https://doi.org/10.21273/HORTTECH.25.5.645

Wang X, Fu X, Chen M, Huan L, Liu W, Qi Y, Gao D (2018) Ultraviolet B irradiation influences the fruit quality and sucrose metabolism of peach (*Prunus persica* L.). Envi and Exp Bot 153:286–301. https://doi.org/10.1016/j.envexpbot.2018.04.015

Wang XT, Xiao JH, Li L, Guo JF, Zhang MX, An YY, He JM (2022) Ethylene acts as a local and systemic signal to mediate UV-B-induced nitrate reallocation to Arabidopsis leaves and roots via regulating the ERFs-NRT1. 8 signaling module. Int J Mol Sci 23:9068. https://doi.org/10.3390/ijms23169068

Xie L, Song Y, Petersen K, Solhaug KA, Lind OC, Brede DA, Tollefsen KE (2022) Ultraviolet B modulates gamma radiation-induced stress responses in Lemna minor at multiple levels of biological organisation. Sci Total Environ 846:157457. https://doi.org/10.1016/j.scitotenv.2022.157457

Xu J, Luo H, Zhou SS, Jiao SQ, Jia KH, Nie S, Mao JF (2022) UV-B and UV-C radiation trigger both common and distinctive signal perceptions and transmissions in Pinus tabuliformis Carr. Tree Phys. https://doi.org/10.1093/treephys/tpac021

Yemm EW, Willis A (1954) The estimation of carbohydrates in plant extracts by anthrone. Biochem J 57(3):508–514

Yu S, Li M, Dubcovsky J, Tian L (2022) Mutant combinations of lycopene ε-cyclase and β-carotene hydroxylase 2 homoeologs increased β-carotene accumulation in endosperm of tetraploid wheat (*Triticum turgidum* L.) grains. Plant Bio J 20(3):564–576. https://doi.org/10.1111/pbi.13738